

ning of a two-dimensional site adsorption (ion "condensation").

One incidental outcome of the above calculations is that nonlinear charge-potential functions can be derived on the basis of linear differential equations (using linear boundary value conditions) by appropriate definitions of boundaries and related boundary values. It therefore appears that experimental observations of nonlinear charge-potential behavior do not *ipso facto* support either the nonlinear Poisson-Boltzmann equation or its linear version.

Conclusions

An ionic adsorption model of an electrical double layer has been derived and applied to calculations of repulsive pressures in clay-water systems. The model can rationalize nearly all the available data to probably within the experimental error over 2 orders of magnitude of pressures and ionic strengths. Unlike the classical double-layer theory, which neglects ionic adsorption phenomena, the model predicts very large repulsions at close double-layer separations. These repulsions are attributed to counterion hydration/dehydration equilibrium close to a charged surface. Therefore the concept of hydration forces that may originate from modified solvent structure in the proximity of a (charged) surface need not be invoked for

these particular experiments. Nevertheless, the present model does not rule out the possibility of such structural forces, the existence of which would be best demonstrated at surfaces near the point of zero charge. The ionic adsorption model also predicts the Stern potential (ζ potential) to be nearly independent of ionic strength, and this prediction appears to be confirmed experimentally. The Gouy-Chapman-Stern theory predicts too strong ionic strength dependence of the ζ potential.

Qualitative calculations with the new model suggest that, unlike the Gouy-Chapman-Stern theory, the differential capacity of an electrical double layer may not be differentiable in respect to surface charge at predicted critical surface charge densities. Such surface phase transitions could be most easily observed at low ionic strengths near the point of zero charge.

Acknowledgment. I thank Prof. D. Dolman, S. F. O'Shea, and Loren Hepler for encouragement and comments and the University of Lethbridge and the Natural Sciences and Engineering Research Council for financial support. Prof. B. A. Pethica, J. N. Israelachvili, J. O'M. Bockris, J. Lyklema, G. S. Manning, C. Tanford, P. F. Low, V. A. Parsegian, R. H. Wood, and H. P. Bennetto are thanked for critical comments.

Aqueous Sodium Halide Solutions of Nonionic and Cationic Surfactants with a Consolute Phase Boundary. Light Scattering Behavior

T. Imae

Department of Chemistry, Faculty of Science, Nagoya University, Chikusa, Nagoya 464, Japan

Received May 25, 1988. In Final Form: September 13, 1988

The static and dynamic light scattering of hepta(oxyethylene) tetradecyl ether ($C_{14}E_7$) in 1 M NaCl, tetradecyldimethylammonium chloride ($C_{14}DAC$) in 2.6 M NaCl, and tetradecyldimethylammonium bromide ($C_{14}DAB$) in 4.3 M NaBr has been measured at various temperatures, and the micelle size and the intermicellar interaction have been evaluated at a finite micelle concentration in the dilute regime. Rodlike micelles grow with a rise in temperature, and an increase in the aggregation number produces a large value of the frictional virial coefficient. Therefore, the negative, large value of the hydrodynamic virial coefficient is raised, while the second virial coefficient of rodlike micelles is small, independent of the temperature. The solution behavior of rodlike micelles in the semidilute regime obeys the scaling laws with the characteristic exponents, ν , of 0.58-0.75 for $C_{14}E_7$ and 0.57-0.63 for $C_{14}DAC$ and $C_{14}DAB$. The angular dependence of the effective diffusion coefficient in the semidilute regime is classified by two types, depending on whether the initial slope is positive or negative. The relation between the threshold micelle concentration of overlap, $(c - c_0)^*$, and the consolute phase boundary is discussed.

Introduction

Aqueous solutions of oligo(oxyethylene) alkyl ethers (C_nE_m) separate into two liquid phases when the temperature rises above the lower consolute phase boundary or the cloud point.¹⁻⁹ The lower consolute temperature

varies, if electrolytes are added to aqueous C_nE_m solutions.¹⁰⁻¹⁴ We have recently reported that aqueous solutions of alkyldimethylammonium chlorides and bromides (C_nDAC , C_nDAB) and dodecylammonium chloride induce the liquid-liquid phase separation when sodium halides

(1) Balmbra, R. R.; Clunie, J. S.; Corkill, J. M.; Goodman, J. F. *Trans. Faraday Soc.* **1962**, *58*, 1661; **1964**, *60*, 979.

(2) Clunie, J. S.; Corkill, J. M.; Goodman, J. F.; Symons, P. C.; Tate, J. R. *Trans. Faraday Soc.* **1967**, *63*, 2839.

(3) Clunie, J. S.; Goodman, J. F.; Symons, P. C. *Trans. Faraday Soc.* **1969**, *65*, 287.

(4) Ekwall, P. *Advances in Liquid Crystals*; Brown, G. H., Ed., Academic: New York, San Francisco, London, 1975; Vol. I, pp 1-142.

(5) Lang, L. C.; Morgan, R. D. *J. Chem. Phys.* **1980**, *73*, 5849.

(6) Mitchell, D. J.; Tiddy, D. J. T.; Waring, L.; Bostock, T.; McDonald, M. P. *J. Chem. Soc., Faraday Trans 1* **1983**, *79*, 975.

(7) Zulauf, M.; Rosenbusch, J. P. *J. Phys. Chem.* **1983**, *87*, 856.

(8) Corti, M.; Minero, C.; Degiorgio, V. *J. Phys. Chem.* **1984**, *88*, 309.

(9) Corti, M.; Minero, C.; Cantù, L.; Piazza, R. *Colloids Surf.* **1984**, *12*, 341.

(10) Maclay, W. N. *J. Colloid Sci.* **1956**, *11*, 272.

(11) Schick, M. J. *J. Colloid Sci.* **1962**, *17*, 801.

(12) Tokiwa, F.; Matsumoto, T. *Bull. Chem. Soc. Jpn.* **1975**, *48*, 1645.

(13) Deguchi, K.; Meguro, K. *J. Colloid Interface Sci.* **1975**, *50*, 223.

(14) Zulauf, M. *Physics of Amphiphiles, Micelles, Vesicles, and Microemulsions*; Degiorgio, V., Corti, M., Eds.; North-Holland: Amsterdam, 1985; p 663.

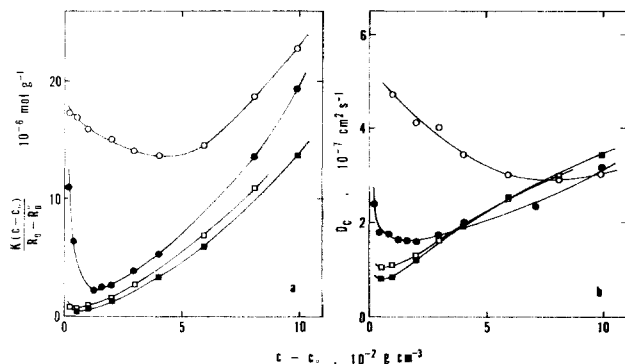


Figure 1. Debye plots and diffusion coefficients at zero scattering angle for 1 M NaCl solutions of $C_{14}E_7$. (a) Debye plot; (b) diffusion coefficient. Temperature ($^{\circ}C$): \circ , 15; \bullet , 25; \square , 35; \blacksquare , 40.

are added to the solutions.¹⁵

The physicochemical properties of aqueous surfactant solutions with a consolute phase boundary have been investigated by several workers. Among their investigations, light scattering and viscosity measurements at various temperatures up to the lower consolute phase boundary have brought important information about the micelle growth and the intermicellar interaction.^{1,7,8,16-24} Moreover, recent works for aqueous sodium halide solutions of C_nE_7 , C_nDAC , and C_nDAB indicated the presence of overlapped and entangled rodlike micelles in homogeneous solutions.²⁵⁻²⁷

The overlap and entanglement of rodlike micelles were first evidenced in semidilute solutions of tetradecylpyridinium *n*-heptanesulfonate²⁸ and cetylpyridinium salicylate,²⁹ and later the analysis based on the scaling laws was applied to aqueous salt solutions of alkyltrimethylammonium halides, C_nDAC , C_nDAB , and C_nEm .^{23,25-27,30-34}

In this work, the static and dynamic light scattering for aqueous sodium halide solutions of $C_{14}E_7$, $C_{14}DAC$, and $C_{14}DAB$ is measured at various temperatures between the lower consolute phase boundary and the Krafft boundary. The size of rodlike micelles and the intermicellar interaction at a finite micelle concentration are evaluated in the dilute regime, and the scaling laws are investigated in the semidilute regime. The threshold micelle concentra-

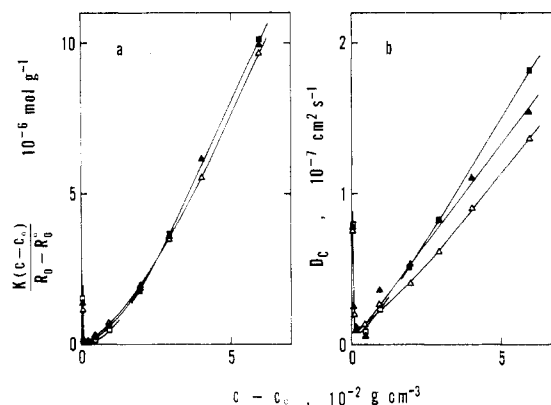


Figure 2. Debye plots and diffusion coefficients at zero scattering angle for 2.6 M NaCl solutions of $C_{14}DAC$. (a) Debye plot; (b) diffusion coefficient. Temperature ($^{\circ}C$): Δ , 20; \blacktriangle , 30; \blacksquare , 40.

tion of overlap is discussed in relation to the consolute phase boundary.

Although measurements of the static and dynamic light scattering are available to analyze the characteristics of large or rodlike micelles, which are formed at finite micelle concentrations,^{30,31,35-37} the solution behavior at finite micelle concentrations should include the intermicellar interaction, besides the micelle growth, and no workers evaluate simultaneously two effects at such concentrations. Recently, the procedure for such an analysis was developed, and the size of nonionic micelles and the intermicellar interaction were calculated.^{25,38} In this work, the same procedure of one concentration method is applied to dilute solutions of $C_{14}E_7$, $C_{14}DAC$, and $C_{14}DAB$.

Experimental Section

Samples of $C_{14}E_7$, $C_{14}DAC$, and $C_{14}DAB$ are the same as previously used.^{15,25-27,38} NaCl and NaBr were ignited for 1 h, and water was redistilled from alkaline $KMnO_4$. The measurements of static and dynamic light scattering and specific refractive index increment were carried out at a 488-nm wavelength on an Otsuka Denshi dynamic light-scattering spectrophotometer DLS-700 and an Otsuka Denshi differential refractometer RM-102, respectively. The temperature was changed from 15 to 45 $^{\circ}C$. The procedure of measurement is described in detail elsewhere.^{25,38,38}

Results

Static and Dynamic Light Scattering. Figure 1 shows the static and dynamic light scattering at zero scattering angle for 1 M NaCl solutions of $C_{14}E_7$. The Debye plots and the diffusion coefficients decrease with increasing micelle concentration and increase through minima at high micelle concentrations. As the temperature rises from 15 to 40 $^{\circ}C$, the Debye plots and the diffusion coefficients decrease and the minima shift to lower micelle concentrations.

As seen in Figure 2, the Debye plots and the diffusion coefficients for 2.6 M NaCl solutions of $C_{14}DAC$ have minima at low micelle concentrations, and they slightly depend on the temperature. Similar features were observed for 4.3 M NaBr solutions of $C_{14}DAB$.

If R and R^0 represent the reduced scattering intensities at the surfactant concentration, c , and the critical micelle concentration, c_0 , respectively, and K is the optical constant, the reciprocal reduced scattering intensity at the

- (15) Imae, T.; Sasaki, M.; Abe, A.; Ikeda, S. *Langmuir* 1988, 4, 414.
 (16) Elworthy, P. H.; McDonald, C. *Kolloid-Z. Z. Polym.* 1964, 195, 16.
 (17) Hayter, J. B.; Zulauf, M. *Colloid Polym. Sci.* 1982, 260, 1023.
 (18) Fujimatsu, H.; Takagi, K.; Matsuda, H.; Kuroiwa, S. *J. Colloid Interface Sci.* 1983, 94, 237.
 (19) Nilsson, P.-G.; Wennerström, H.; Lindman, B. *J. Phys. Chem.* 1983, 87, 1377.
 (20) Zana, R.; Weill, C. *J. Phys. Lett.* 1985, 46, L-953.
 (21) Zulauf, M.; Weckström, K.; Hayter, J. B.; Degiorgio, V.; Corti, M. *J. Phys. Chem.* 1985, 89, 3411.
 (22) Kato, T.; Seimiya, T. *J. Phys. Chem.* 1986, 90, 3159.
 (23) Kato, T.; Anzai, S.; Seimiya, T. *J. Phys. Chem.* 1987, 91, 4655.
 (24) Wilcoxon, J. P.; Kaler, E. W. *J. Chem. Phys.* 1987, 86, 4684.
 (25) Imae, T. *J. Phys. Chem.* 1988, 92, 5721.
 (26) Imae, T.; Sasaki, M.; Ikeda, S. *J. Colloid Interface Sci.* 1989, in press.
 (27) Sasaki, M.; Imae, T.; Ikeda, S. *Langmuir*, following paper in this issue.
 (28) Hoffmann, H.; Rehage, H.; Platz, G.; Schorr, W.; Thurn, H.; Ulbricht, W. *Colloid Polym. Sci.* 1982, 260, 1042.
 (29) Hoffmann, H.; Platz, G.; Rehage, H.; Schorr, W. *Adv. Colloid Interface Sci.* 1982, 17, 275.
 (30) Candau, S. J.; Hirsh, E.; Zana, R. *J. Phys. (Les Ulis, Fr.)* 1984, 45, 1263.
 (31) Candau, S. J.; Hirsh, E.; Zana, R. *J. Colloid Interface Sci.* 1985, 105, 521.
 (32) Imae, T.; Ikeda, S. *J. Phys. Chem.* 1986, 90, 5216.
 (33) Imae, T.; Ikeda, S. *Colloid Polym. Sci.* 1987, 265, 1090.
 (34) Imae, T.; Abe, A.; Ikeda, S. *J. Phys. Chem.* 1988, 92, 1548.

- (35) Young, C. Y.; Missel, P. J.; Mazer, N. A.; Benedeck, G. B.; Carey, M. C. *J. Phys. Chem.* 1978, 82, 1375.
 (36) Appell, J.; Porte, G. *J. Colloid Interface Sci.* 1981, 81, 85.
 (37) Appell, J.; Porte, G.; Poggi, Y. *J. Colloid Interface Sci.* 1982, 87, 492.
 (38) Imae, T. *J. Colloid Interface Sci.* 1988, in press.

Table I. Characteristics of Rodlike Micelles in Aqueous Sodium Halide Solutions at Various Temperatures

$T, ^\circ\text{C}$	$(\partial\bar{n}/\partial c)_{C_s}$, $\text{cm}^3 \text{g}^{-1}$	$10^{-4}M_{\text{app}}$, g mol^{-1}	m_{app}	$R_{G,\text{app}}$, nm	$R_{H,\text{app}}$, nm	ρ_{app}
C ₁₄ E ₇ in 1 M NaCl						
15	0.127	7.32	140		5.0	
25	0.134 ^a	44.1	844	24.4	14.9	1.64
35	0.119	146	2790	43.0	27.1	1.59
40	0.112	287	5490	66.6	39.9	1.67
C ₁₄ DAC in 2.6 M NaCl						
20	0.126	895	39 300	177	140	1.26
30	0.126	1250	44 900	195	185	1.05
35	0.126 ^a					
40	0.124					
C ₁₄ DAB in 4.3 M NaBr						
25	0.098 ₀	1100	34 200	181	169	1.07
30	0.087 ₇ ^a	1770	54 900	206	190	1.08
35	0.081 ₂	2960	92 000	250	245	1.02
45	0.074 ₄					

^a Interpolated values.

scattering angle θ and the effective diffusion coefficient at 0° direction are written as

$$K(c - c_0)/(R_\theta - R_\theta^0) = (1/M_{\text{app}})[1 + (1/3)R_{G,\text{app}}^2\mu^2] \quad (1)$$

$$D_c = k_B T / 6\pi\eta_0 R_{H,\text{app}} \quad (2)$$

respectively, at small $R_{G,\text{app}}^2\mu^2$ for dilute solutions of micelles. M , R_G , and R_H are the molecular weight, radius of gyration, and hydrodynamic radius of micelles, respectively, and the subscript app implies "apparent". μ is the magnitude of the scattering vector, k_B is the Boltzmann constant, T is the absolute temperature, and η_0 is the viscosity of solvent.

The apparent molecular weight, radius of gyration, and hydrodynamic radius of C₁₄E₇, C₁₄DAC, and C₁₄DAB micelles in aqueous sodium halide solutions can be obtained at the micelle concentration, at which the reciprocal reduced scattering intensity is minimum and the apparent micelle molecular weight is maximum. The numerical values are given in Table I. In Table I, the apparent micelle aggregation number, $m_{\text{app}} = M_{\text{app}}/M_1$, is included with the values of $\rho_{\text{app}} \equiv R_{G,\text{app}}/R_{H,\text{app}}$ and of the specific refractive index increment, $(\partial\bar{n}/\partial c)_{C_s}$, at a constant salt concentration, C_s (M), where \bar{n} is the refractive index of solution and M_1 is the molecular weight of a surfactant molecule.

Since the apparent micelle aggregation number ranges from 140 to 5490 for C₁₄E₇ and from 34 200 to 92 000 for C₁₄DAC and C₁₄DAB, it is suggested that rodlike micelles are formed in all solutions examined here. Although C₁₄E₇ micelles are smaller than C₁₄DAC and C₁₄DAB micelles, the micelle size increases largely for C₁₄E₇ and slightly for C₁₄DAC and C₁₄DAB, as the temperature rises. The apparent radius of gyration is larger than the apparent hydrodynamic radius, but both increase with an increase in the apparent aggregation number.

Micelle Size and Intermicellar Interaction. When the characteristics of micelles are examined at the finite micelle concentration, the intermicellar interaction should be considered, besides the micelle growth. Then the equations

$$K(c - c_0)/(R_\theta - R_\theta^0) = (1/M)[1 + (1/3)R_G^2\mu^2] + 2B_2(c - c_0) \quad (3)$$

$$D = D_c[1 + AR_G^2\mu^2] \quad (4)$$

$$D_c = D_0[1 + k_D(c - c_0)] \quad (5)$$

$$D_0 = k_B T / 6\pi\eta_0 R_H \quad (6)$$

hold for dilute solutions of rodlike micelles, instead of eq 1 and 2. B_2 is the second virial coefficient, k_D is the hydrodynamic virial coefficient, and A is the coefficient, which is evaluated as $2/15$ for linear chains.^{39,40}

The coefficient, k_D , is described by⁴¹

$$k_D = 2B_2M - k_f - \bar{v} \quad (7)$$

with the frictional virial coefficient

$$k_f = (k_B T / D_0 \eta_0)(B_2^2 N_A M / 12\pi^2)^{1/3} \quad (8)$$

for rod particles.⁴² \bar{v} is the partial specific volume of a particle, and N_A is Avogadro's number.

According to the procedure previously described²⁵ and utilizing the \bar{v} values of homologues in the literature,^{32,43} the numerical values of various characteristic parameters for rodlike micelles in aqueous sodium halide solutions are evaluated from the angular dependence of the reciprocal reduced scattering intensity and the effective diffusion coefficient. The numerical values for the micellar solutions at the minimum of the reciprocal reduced scattering intensity are listed in Table II.

While the aggregation number, radius of gyration, and hydrodynamic radius for rodlike micelles of C₁₄E₇ in 1 M NaCl are smaller than those of C₁₄DAC in 2.6 M NaCl and C₁₄DAB in 4.3 M NaBr, three kinds of rodlike micelles become larger with a rise in temperature. The second virial coefficient of rodlike micelles scarcely depends on the temperature, the sort of surfactants, and the added salt concentration. The numerical values are 1.65×10^{-5} mol cm³ g⁻² or less.

Depending on the increase in micelle size, the frictional virial coefficient of rodlike micelles increases, as expected from eq 8. The numerical values vary from 24 to 32 cm³ g⁻¹ for C₁₄E₇ in 1 M NaCl and range from 190 to 430 cm³ g⁻¹ for C₁₄DAC in 2.6 M NaCl and C₁₄DAB in 4.3 M NaBr, as the temperature rises.

The hydrodynamic virial coefficient of rodlike micelles exhibits negative values between -7 and -17 cm³ g⁻¹ for C₁₄E₇ and between -110 and -150 cm³ g⁻¹ for C₁₄DAC and C₁₄DAB, indicating that the frictional virial coefficient strongly contributes to the hydrodynamic virial coefficient.

The dimensionless quantity $\rho \equiv R_G/R_H$ is calculated and listed in Table II. The ρ values are between 1.57 and 1.97, which are larger than 1.3-1.7 for flexible linear polymers⁴⁴⁻⁴⁶ and smaller than 2.9 for a fairly rigid rod.⁴² Therefore, rodlike micelles of C₁₄E₇, C₁₄DAC, and C₁₄DAB may be regarded as semiflexible.

Overlapped and Entangled Rodlike Micelles in Semidilute Solutions. The threshold micelle concentration where rodlike micelles overlap with one another is defined by⁴⁷

$$(c - c_0)^* \approx M / [(4/3)\pi R_G^3 N_A] \quad (9)$$

The solutions of rodlike micelles are classified into two regimes, dilute and semidilute regimes, by this charac-

(39) Burchard, W.; Schmidt, M.; Stockmayer, W. H. *Macromolecules* 1980, 13, 580.

(40) Burchard, W. *Adv. Polym. Sci.* 1983, 48, 1.

(41) Yamakawa, H. *Modern Theory of Polymer Solution*; Harper and Row: New York, 1971; p 181.

(42) Kubota, K.; Tominaga, Y.; Fujime, S. *Macromolecules* 1986, 19, 1604.

(43) Güveli, D. E.; Davis, S. S.; Kayes, J. B. *J. Colloid Interface Sci.* 1983, 91, 1.

(44) Schmidt, M.; Burchard, W. *Macromolecules* 1981, 14, 210.

(45) Tsunashima, Y.; Nemoto, N.; Kurata, M. *Macromolecules* 1983, 16, 1184.

(46) Kato, T.; Katsuki, T.; Takahashi, A. *Macromolecules* 1984, 17, 1726.

(47) Cotton, J. P.; Nierlich, M.; Boue, F.; Daoud, M.; Farnoux, B.; Jannink, G.; Duplessix, R.; Picot, C. *J. Chem. Phys.* 1976, 65, 1101.

Table II. Characteristics of Rodlike Micelles in Aqueous Sodium Halide Solutions at Various Temperatures

$T, ^\circ\text{C}$	$10^{-4} M, \text{g mol}^{-1}$	m	R_G, nm	R_H, nm	ρ	$10^6 B_{2, \text{rod}}, \text{mol cm}^3 \text{g}^{-2}$	$10^6 B_{2, \text{rod}}, \text{mol cm}^3 \text{g}^{-2}$	$k_T, \text{cm}^3 \text{g}^{-1}$	$k_D, \text{cm}^3 \text{g}^{-1}$	$10^2(c - c_0), \text{g cm}^{-3}$
C_{14}E_7 in 1 M NaCl										
25	54.1	1040	27.1	13.7	1.97	1.65	10.2	23.5	-6.6	1.08
35	164	3040	44.9	25.2	1.78	0.53	3.06	29.0	-13.2	0.70
40	334	5960	69.4	36.4	1.91	0.25	1.76	32.3	-17.4	0.37
C_{14}DAC in 2.6 M NaCl										
20	1020	37600	191	108	1.77	0.40	0.84	191	-109	0.06
30	1870	66100	237	128	1.84	0.63	0.38	382	-150	0.06
C_{14}DAB in 4.3 M NaBr										
25	1710	53000	226	124	1.82	0.84	0.46	426	-140	0.06
30	2300	69600	232	141	1.64	0.31	0.27	274	-135	0.07
35	3800	114000	278	177	1.57	0.17	0.14	270	-147	0.07

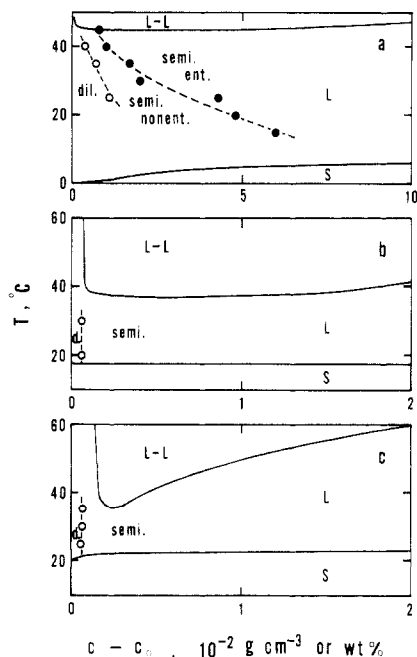


Figure 3. Threshold micelle concentrations of overlap and entanglement and the phase diagrams as a function of the temperature. (a) C_{14}E_7 in 1 M NaCl; (b) C_{14}DAC in 2.6 M NaCl; (c) C_{14}DAB in 4.3 M NaBr. \circ , threshold micelle concentration of overlap; \bullet , threshold micelle concentration of entanglement (ref 26). The phase diagrams (ref 15) are drawn by the concentrations of wt %. L-L, two-liquid-phase region; L, homogeneous region; s, solid region.

teristic micelle concentration. Table II includes the numerical values of $(c - c_0)^*$, and Figure 3 illustrates them as a function of the temperature. Whereas the overlap threshold values of rodlike micelles of C_{14}E_7 decrease with a rise in temperature, those of C_{14}DAC and C_{14}DAB are $(0.06\text{--}0.07) \times 10^{-2} \text{g cm}^{-3}$, independent of the temperature. The overlap threshold values are very close to the micelle concentrations, at which the reciprocal reduced scattering intensities are minimum.

The solution properties of rodlike micelles in a semidilute regime can be described by the scaling laws as similar to those for overlapped and entangled polymer chains.⁴⁸ Then the scaling laws for overlapped and entangled rodlike micelles may be written

$$K(c - c_0)/(R_0 - R_0^0) \sim (c - c_0)^{1/(3\nu_G - 1)} \quad (10)$$

and

$$D_c \sim (c - c_0)^{\nu_H/(3\nu_H - 1)} \quad (11)$$

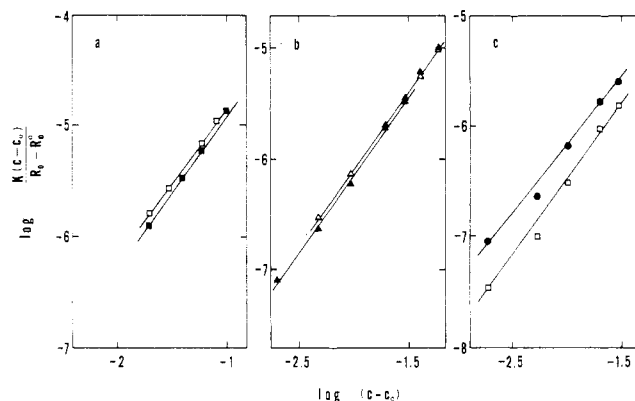


Figure 4. Double-logarithmic plots of the reciprocal reduced scattering intensity at zero scattering angle vs micelle concentration for semidilute solutions of surfactants. (a) C_{14}E_7 in 1 M NaCl; (b) C_{14}DAC in 2.6 M NaCl; (c) C_{14}DAB in 4.3 M NaBr. The symbols represent the same temperatures as in Figures 1 and 2.

Table III. Scaling Laws for Semidilute Micelle Solutions at Different Temperatures

$T, ^\circ\text{C}$	ν_G	ν_H
C_{14}E_7 in 1 M NaCl		
35	0.58	0.75
40	0.58	0.74
C_{14}DAC in 2.6 M NaCl		
20	0.58	0.57
30	0.57	0.53
C_{14}DAB in 4.3 M NaBr		
25	0.60	0.59
35	0.58	0.63

against micelle concentrations, where ν_G and ν_H are the characteristic exponents in the relations of

$$R_G \sim m^{\nu_G} \quad (12)$$

and

$$R_H \sim m^{\nu_H} \quad (13)$$

that is, in the scaling laws in dilute solutions.

Figures 4 and 5 give the double-logarithmic plots of light-scattering data from semidilute micelle solutions as a function of the micelle concentration, according to eq 10 and 11. The linear relation holds for all systems. The characteristic exponents are evaluated from the slopes of the straight lines and listed in Table III.

The ν values for semidilute micelle solutions are in the range 0.58–0.75 for C_{14}E_7 and 0.57–0.63 for C_{14}DAC and C_{14}DAB , independent of the temperature. The ν values from static and dynamic light scattering are consistent with each other.

(48) de Gennes, P.-G. *Scaling Concepts in Polymer Physics*; Cornell University Press: Ithaca, London, 1979.

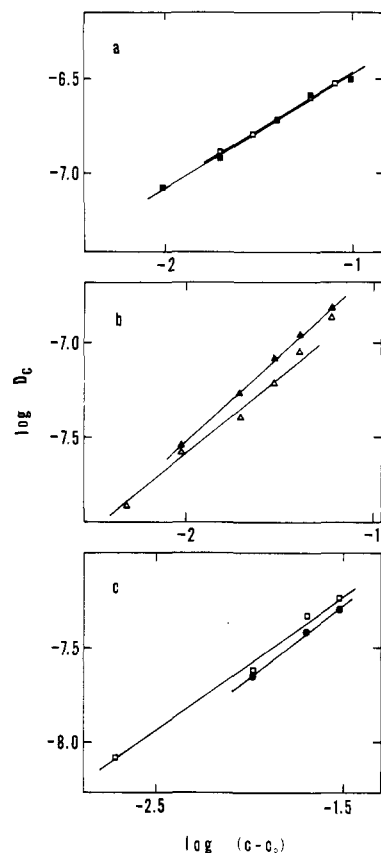


Figure 5. Double-logarithmic plots of the effective diffusion coefficient at zero scattering angle vs micelle concentration for semidilute solutions of surfactants. (a) $C_{14}E_7$ in 1 M NaCl; (b) $C_{14}DAC$ in 2.6 M NaCl; (c) $C_{14}DAB$ in 4.3 M NaBr. The symbols represent the same temperatures as in Figures 1 and 2.

Angular Dependence of Dynamic Light Scattering.

Figure 6 represents the angular dependence of the effective diffusion coefficients for 2.6 M NaCl solutions of $C_{14}DAC$ at 20 °C. When the micelle concentrations are low, the effective diffusion coefficients at low scattering angles increase linearly with a positive slope, as the $\sin^2(\theta/2)$ values increase. While the linearity holds even at high scattering angles for solutions with micelle concentrations of 0.095 and $0.20 \times 10^{-2} \text{ g cm}^{-3}$, the effective diffusion coefficients for solutions of $0.48 \times 10^{-2} \text{ g cm}^{-3}$ deviate downward from a straight line at high angles.

At high micelle concentrations, the effective diffusion coefficients steeply decrease with first increasing scattering angle. With further increase in scattering angle, the effective diffusion coefficients increase through a minimum for solutions of 0.95 and $1.94 \times 10^{-2} \text{ g cm}^{-3}$, whereas those for solutions above $2.93 \times 10^{-2} \text{ g cm}^{-3}$ become constant at high scattering angles.

For $C_{14}DAC$ in 2.6 M NaCl at 30–40 °C and $C_{14}DAB$ in 4.3 M NaBr at 25–45 °C, solutions with low micelle concentrations reveal a positive straight line at low angles and a downward deviation from it at high angles, while curvatures with a negative slope at low angles are obtained for solutions with high micelle concentrations. The crossover between two types of the angular dependence is $(0.5\text{--}1.0) \times 10^{-2} \text{ g cm}^{-3}$ for $C_{14}DAC$ and $C_{14}DAB$, independent of the temperature.

NaCl solutions (1 M) of $C_{14}E_7$ with micelle concentrations of $(0.81\text{--}9.93) \times 10^{-2} \text{ g cm}^{-3}$ at 25 °C, $(0.21\text{--}5.95) \times 10^{-2} \text{ g cm}^{-3}$ at 35 °C, and $(0.54\text{--}2.00) \times 10^{-2} \text{ g cm}^{-3}$ at 40 °C exhibit the linear relation of the effective diffusion coefficients against $\sin^2(\theta/2)$. The solutions of $8.12 \times 10^{-2} \text{ g cm}^{-3}$ at 35 °C and $(4.04\text{--}9.93) \times 10^{-2} \text{ g cm}^{-3}$ at 40 °C

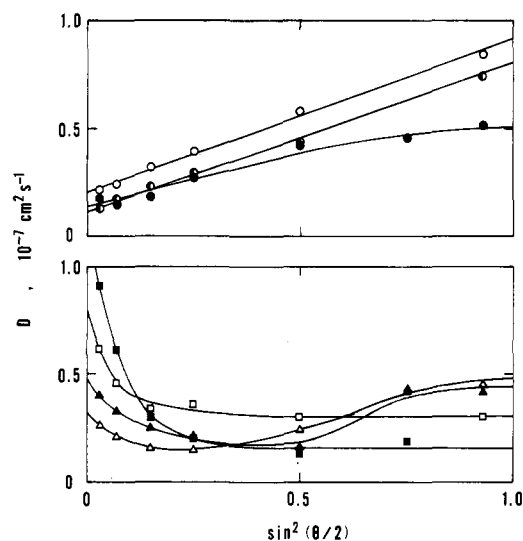


Figure 6. Angular dependence of the effective diffusion coefficients for 2.6 M NaCl solutions of $C_{14}DAC$ at 20 °C. Micelle concentration ($10^{-2} \text{ g cm}^{-3}$): \circ , 0.095; \bullet , 0.203; \bullet , 0.483; Δ , 0.946; Δ , 1.94; \square , 2.93; \blacksquare , 4.03.

present negative slopes over whole scattering angles.

In the previous section, the characteristics of rodlike micelles are evaluated at the finite micelle concentrations, at which the reciprocal reduced scattering intensity is minimum. These concentrations are within the region where the angular dependence of the effective diffusion coefficient has the positive straight line, at least at low scattering angles. Therefore, eq 4 holds at small $R_G^2\mu^2$ for the corresponding solutions.

Discussion

The light scattering was measured for aqueous sodium halide solutions of $C_{14}E_7$, $C_{14}DAC$, and $C_{14}DAB$. The reciprocal reduced scattering intensities and the effective diffusion coefficients display minima around the threshold micelle concentration, above which rodlike micelles overlap with one another. The size of rodlike micelles and the intermicellar interaction were evaluated at a micelle concentration where the reciprocal reduced scattering intensity is minimum or the apparent micelle aggregation number is largest.

The aggregation number, radius of gyration, and hydrodynamic radius of rodlike micelles increase with an increase in temperature. The frictional virial coefficient increases strongly with the micelle size, and, hence, the hydrodynamic virial coefficient becomes negative and large. On the other hand, the second virial coefficient of rodlike micelles is small, independent of the temperature and the micelle aggregation number.

Since a large amount of sodium halide is added to aqueous solutions of $C_{14}DAC$ and $C_{14}DAB$, the intermicellar electrostatic repulsion force should be depressed in these solutions. Then the steric repulsion from the intermicellar excluded volume mainly contributes to the second virial coefficient. The second virial coefficient for rigid rod particles can be evaluated from the equation⁴⁹

$$B_{2,\text{rod}} = 6\pi N_A r R_G^2 / M^2 \quad (14)$$

utilizing the relation $R_G^2 = L^2/12$, where r and L are the radius and the contour length of a rigid rod, respectively.

The numerical values of $B_{2,\text{rod}}$ for rodlike micelles of $C_{14}E_7$, $C_{14}DAC$, and $C_{14}DAB$ are calculated and listed in

(49) Zimm, B. H. *J. Chem. Phys.* 1946, 14, 164.

Table II. In the calculation, the r values of 3.6, 2.1, and 2.3 nm are adopted for micelles of three surfactants, respectively, by estimating from those of analogous surfactant micelles.^{32,38} For C₁₄DAC and C₁₄DAB micelles, the second virial coefficients based on steric repulsion of rods are comparable to the values evaluated from the observed light-scattering data.

It may be concluded that the effective diffusion coefficients of long rodlike micelles are contributed by a negative and large hydrodynamic interaction, while the reciprocal reduced scattering intensities include a very small contribution of the intermicellar interaction, if the large amount of salt is added.

The semidilute solutions of overlapped and entangled rodlike micelles can be analyzed on the basis of the scaling laws. The characteristic exponents, ν , evaluated from light-scattering data in semidilute regime are 0.58–0.75 for C₁₄E₇ and 0.57–0.63 for C₁₄DAC and C₁₄DAB, independent of the temperature and consistent with static and dynamic light scattering.

The characteristic exponents of rodlike micelles were obtained for cationic and nonionic micelles in aqueous solutions with different sodium halide concentrations. The ν_G values were 0.54–0.55 for alkyltrimethylammonium halides^{32,33} and 0.70 for oleyldimethylamine oxide.⁵⁰ The ν_G and ν_H values for hepta(oxyethylene) alkyl ethers were evaluated as 0.58–0.71, independent of NaCl concentration and alkyl chain length.²⁵ The ν values of C_nE₇, C₁₄DAC, and C₁₄DAB are larger than those of alkyltrimethylammonium halides but lower than those of oleyldimethylamine oxide.

As seen in Figure 3, the threshold micelle concentrations of overlap for C₁₄E₇ micelles in 1 M NaCl decrease with an increase in temperature, while those for C₁₄DAC in 2.6 M NaCl and C₁₄DAB in 4.3 M NaBr are independent of the temperature.

In Figure 3, the threshold micelle concentrations of entanglement for C₁₄E₇ micelles in 1 M NaCl are plotted. Such concentrations were obtained from viscometric measurement²⁶ and represent the threshold values above which rodlike micelles entangle. Although the threshold micelle concentrations of entanglement also decrease with an increase in temperature, there exists the serious discrepancy between the threshold values of overlap and entanglement, implying that the entanglement of rodlike micelles occurs at higher micelle concentrations than the overlap. The same discrepancy was obtained for aqueous NaBr solutions of hexadecyltrimethylammonium bromide.³⁴

The phase diagrams for aqueous sodium halide solutions of C₁₄E₇, C₁₄DAC, and C₁₄DAB¹⁵ are illustrated in Figure 3. The liquid–liquid phase separation occurs at high

temperatures, and the homogeneous solutions nearby the lower consolute temperatures are within the semidilute regime. The crossover concentration between dilute and semidilute regimes nearby the lower consolute temperature is close to the micelle concentration for the lower critical solution temperature or the lower critical solution concentration. However, there is no reason to infer that the occurrence of overlapped rodlike micelles is directly related to the liquid–liquid phase separation.

The angular dependence of the effective diffusion coefficient for aqueous surfactant solutions was reported by few workers. Wilcoxon and Kaler²⁴ revealed that the effective diffusion coefficients for a C₁₂E₆ solution of 1.3×10^{-2} g cm⁻³ at several temperatures increased with an upward convex curvature, as μ^2 increases. Flamberg and Pecora⁵¹ measured the dynamic light scattering for 4 M NaCl solutions of dodecyldimethylammonium chloride. Measurement was carried out at several scattering angles, and results were analyzed on the basis of the scattering theory for very large molecules.

The theoretical formulation of the dynamic light scattering for dilute and semidilute solutions of very large molecules shaped like rigid rods, semiflexible chains, and random coils was performed by Pecora et al.^{52–54} and Fujime and Maeda.^{55–57}

Two types of the angular dependence of the effective diffusion coefficient were detected for aqueous sodium halide solutions of C₁₄E₇, C₁₄DAC, and C₁₄DAB. The angular dependence is conspicuous for solutions of micelle concentrations nearby or more than the threshold value of overlap, $(c - c_0)^*$. At the micelle concentrations of $(c - c_0)^* \lesssim c - c_0 \lesssim 10(c - c_0)^*$, the effective diffusion coefficients increase with an increase in scattering angle, while their initial slopes are negative for solutions of $10(c - c_0)^* \lesssim c - c_0$.

Since rodlike micelles of C₁₄E₇, C₁₄DAC, and C₁₄DAB are semiflexible, as estimated from the observed ρ and ν values, the theoretical analysis of the angular-dependent dynamic light scattering for aqueous solutions of rodlike micelles in the present work must be performed on the basis of the treatment for semiflexible polymer chains in semidilute solutions. Such treatment will be reported in the following paper in this issue.

Registry No. C₁₄E₇, 40036-79-1; C₁₄DAC, 2016-47-9; C₁₄DAB, 64183-88-6; NaCl, 7647-14-5; NaBr, 7647-15-6.

(51) Flamberg, A.; Pecora, R. *J. Phys. Chem.* **1984**, *88*, 3026.

(52) Berne, B. J.; Pecora, R. *Dynamic Light Scattering*; Wiley: New York, 1976.

(53) Zero, K. M.; Pecora, R. *Macromolecules* **1982**, *15*, 87.

(54) Aragóns, S. R.; Pecora, R. *Macromolecules* **1985**, *18*, 1868.

(55) Maeda, T.; Fujime, S. *Macromolecules* **1984**, *17*, 2381.

(56) Fujime, S.; Maeda, T. *Macromolecules* **1985**, *18*, 191.

(57) Fujime, S.; Takasaki-Ohsita, M.; Maeda, T. *Macromolecules* **1987**, *20*, 1292.

(50) Imae, T.; Ikeda, S. *Colloid Polym. Sci.* **1985**, *263*, 756.